

Small-scale topographically-controlled glacier flow switching in an expanding proglacial lake at Breiðamerkurjökull, SE Iceland

STORRAR, Robert <<http://orcid.org/0000-0003-4738-0082>>, JONES, Andrew and EVANS, David J A

Available from Sheffield Hallam University Research Archive (SHURA) at:

<http://shura.shu.ac.uk/15448/>

This document is the author deposited version. You are advised to consult the publisher's version if you wish to cite from it.

Published version

STORRAR, Robert, JONES, Andrew and EVANS, David J A (2017). Small-scale topographically-controlled glacier flow switching in an expanding proglacial lake at Breiðamerkurjökull, SE Iceland. *Journal of Glaciology*, 745-750.

Copyright and re-use policy

See <http://shura.shu.ac.uk/information.html>

Letter

Small-scale topographically-controlled glacier flow switching in an expanding proglacial lake at Breiðamerkurjökull, SE Iceland

1. INTRODUCTION

Understanding the internal dynamics of glaciers and ice sheets is important for predicting how they will respond to external forcing factors, such as rising sea level and warming ocean and air temperatures (e.g. Weertman, 1974; Thomas, 1979; Conway and others, 2002; Pfeffer, 2007; Favier and others, 2014; Aschwanden and others, 2016). Flow switching, where the trajectory of ice flow significantly alters in time, has been inferred in modern ice sheets (e.g. Retzlaff and Bentley, 1993; Jacobel and others, 1996; Anandakrishnan and Alley, 1997; Conway and others, 2002; Hulbe and Fahnestock, 2004) and reconstructed in palaeo-ice sheets (e.g. Dowdeswell and others, 2006; Stokes and others, 2009; Ó Cofaigh and others, 2010; Stokes and Tarasov, 2010; Winsborrow and others, 2012; Stokes and others, 2014). Flow switching is associated with changes in ice dynamics (e.g. Payne and Dongelmans, 1997; Conway and others, 2002) and could lead to either increases or decreases in velocity. It is therefore of importance to future mass-balance predictions, although few examples of flow switches taking place in modern glaciers have been documented. This letter documents the first observation of a minor flow switch as it happens and provides strong support for a topographic (bathymetric) control.

Winsborrow and others (2012) reviewed the literature and proposed five mechanisms that may control flow switching: (1) accumulation of sediment causing accommodation space to be filled (Dowdeswell and others, 2006); (2) variations in bathymetry causing asynchronous response of ice flow (Stokes and others, 2009); (3) variations in basal thermal regime (Ó Cofaigh and others, 2010); (4) variations in subglacial meltwater routing and sticky spot location (Anandakrishnan and Alley, 1997); and (5) large-scale changes in mass balance (Payne and Dongelmans, 1997). All research into flow switching to date has been carried out on flow switches that have occurred in the past, from scales ranging from the last 150 years (Retzlaff and Bentley, 1993) to several glacial cycles (Dowdeswell and others, 2006). Here we document observations of an active small-scale flow switch that is under way at Breiðamerkurjökull, SE Iceland.

2. BREIÐAMERKURJÖKULL

Breiðamerkurjökull is a large (~16 km wide) outlet glacier draining part of the Vatnajökull ice cap in south-east Iceland (Fig. 1). The glacier is composite, comprising four flow units (1–4 from west to east: see Fig. 1a), which are separated by large medial moraines emanating from prominent nunataks. In this paper we focus on the interaction between flow units 3 and 4. The western portion of flow unit 4 terminates in a large proglacial lake named Jökulsárlón and is bounded to the west by a medial moraine named Esjufjallarond. The foreland in this area

rises to no more than 50 m above sea level, the most prominent topographic feature of the area being a large trench up to 300 m deep beneath Jökulsárlón, which extends up-glacier for 20 km (Björnsson, 1996; Björnsson and others, 2001; Fig. 1b). Breiðamerkurjökull has retreated ~6 km since its Little Ice Age maximum position in 1890 and the ice margin is currently retreating over the deepest part of the Jökulsárlón trench (Fig. 1b). Mapping of the glacier and its foreland in 1998 by Evans and Twigg (2002) revealed a depression in the ice surface in the vicinity of the deepest part of the Jökulsárlón trench, which is clearly visible in Figure 2a as an area of low ice-surface topography and dense arcuate crevassing.

3. METHODS

Mean annual surface velocity and flow vectors were calculated using an automated normalised cross-correlation feature tracking algorithm (Kääb and Vollmer, 2000). Values were derived from the panchromatic band (15 m resolution) of a pair of Landsat 7 ETM+ scenes (7 October 1999 and 23 September 2000) and a pair of Landsat 8 OLI scenes (8 October 2014 and 25 September 2015).

Individual vertical aerial photographs were used to derive orthophotos and DEMs for 1998 and 2007 using Structure from Motion photogrammetry. The 1998 DEM is 5 m horizontal resolution and is based on the aerial photographs and control points from the (22 August) 1998 glacial geomorphological map of Breiðamerkurjökull (Evans and Twigg, 2000). The 2007 DEM is 1 m resolution and is based on high resolution (30 cm) NERC ARSF aerial photographs from 3 July 2007 and control points measured in the field (see Storrar and others, 2015 for details). A 2 m DEM from 10 November 2015, produced by photogrammetry from high-resolution (~0.5 m) optical imagery, was acquired from the ArcticDEM (<http://pgc.umn.edu/arcticdem>).

Analysis of the terrestrial component of the 2015 DEM reveals that it is horizontally offset from the 1998 and 2007 DEMs by 7 m. It is systematically vertically offset by ~68 m, varying by a range of ~2 m either side of this value. Thus, to measure surface changes, all DEMs were resampled to 50 m horizontal resolution, to conservatively remove any artefact of error in georeferencing. The elevation values of the 2015 DEM were reduced by 68 m to correct for the systematic error. We estimate that the vertical accuracy of the DEMs is ±5 m. Given that the temporal difference between DEMs is 8–17 years, the vertical uncertainty becomes less significant (<1 m a⁻¹) when calculating surface elevation change between years, which was carried out for 1998–2007, 2007–15 and 1998–2015.

A combination of Landsat 4TM, 5TM, 7ETM+ and 8OLI satellite images of the study area from 1985 to 2016 were downloaded from the USGS (<http://earthexplorer.usgs.gov/>). The temporal resolution is approximately annual from 1985 to 2011, and then monthly (excluding winter) from 2011 to 2016 (details of individual images are provided in the supplementary information). The glacier margin and lateral boundaries of the Esjufjallarond medial moraine were digitised from false colour composite images in the band combination 7, 3, 2 (RGB).

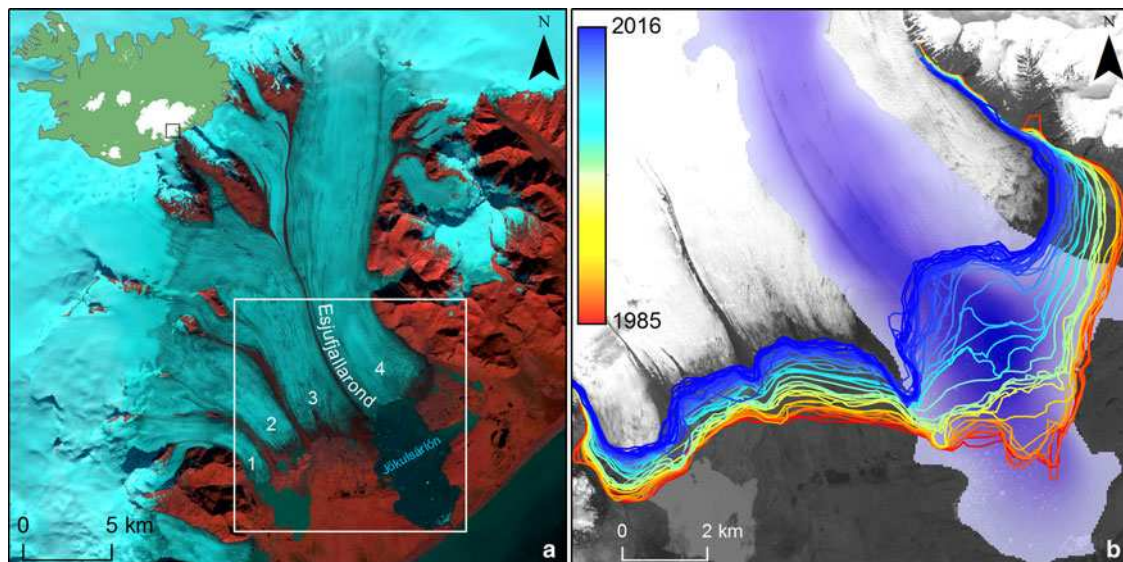


Fig. 1. (a) 2016 Landsat 8 ETM+ image (7, 3, 2 RGB) showing the location of Breiðamerkurjökull and places referred to in the text. Numbers refer to the flow units. The white box indicates the extent of b. (b) Retreat of Breiðamerkurjökull from 1985 to 2016 superimposed on the elevation of the Jökulsárlón trench, which extends down to deeper shades of blue at ~ 300 m below sea level (interpolated from contours provided in Björnsson, 1996).

Maps of subglacial hydraulic potential were derived using a GIS approach similar to that of Livingstone and others (2013), which is based on Shreve (1972). Subglacial hydraulic potential (Φ) is derived from elevation and water pressure:

$$\Phi = \rho_w g h + P_w \quad (1)$$

where ρ_w is the density of water (1000 kg m^{-3}), g is the acceleration due to gravity (9.81 m s^{-2}), h is the elevation of the bed and P_w is the water pressure. Effective pressure N is the difference between ice pressure P_i (917 kg m^{-3}) and subglacial water pressure P_w .

$$N = P_i - P_w \quad (2)$$

P_i is controlled by the weight of overlying ice:

$$P_i = \rho_i g H \quad (3)$$

where H is the ice thickness (m). For simplicity N is assumed to be 0, although this is often not the case, particularly close to the ice margin (cf. Hooke, 1984). However, this simplification is frequently adopted to approximate the generalised pattern of subglacial water flow (e.g. Shreve, 1972; Syverson and others, 1994; Livingstone and others, 2013), which is the aim in this study. Assuming N to be 0, Eqn (1) can be re-written as:

$$\Phi = \rho_w g h + \rho_i g H \quad (4)$$

We use the 1998, 2007 and 2015 DEMs for the ice surface, and a DEM interpolated from the subglacial contours published in Björnsson and others (2001) to derive H and, in turn, Φ . The DEMs were resampled to 200 m resolution to remove the (short-term) effect of ice thickness fluctuations due to crevasses.

4. RESULTS

Mean ice-surface velocity and flow-line patterns (Figs 2a, b) show that areas of higher velocity are generally associated

with the deeper parts of the bed. Between 1999–2000 and 2014/15 the fastest flowing parts of the glacier migrated to the west, and a small net increase in velocity was observed in flow unit 4 (Fig. 2c). The direction of flow changed from broadly NW to SE to NNW to SSE, the changes being most notable near to the terminus.

Ice-surface lowering is concentrated around the deepest parts of the Jökulsárlón trench that are coincident with the ice margin (Figs 2d–i). Between 1998 and 2007 this was further to the east than between 2007 and 2015, where the locus of maximum surface lowering was further west. Rates of ice-surface lowering increased after 2007.

Since 1985, Breiðamerkurjökull has undergone asynchronous retreat, with the fastest retreat occurring over the deepest parts of the Jökulsárlón trench (Fig. 1b; Supplementary animation), coincident with the loci of ice-surface lowering. In 1985 the medial moraine Esjufjallarond followed a straight trajectory and terminated on land to the west of Jökulsárlón (Fig. 3b; Supplementary animation). In 2006, a portion of Esjufjallarond close to the terminus began to deflect towards the north-east, indicating flow capture (Fig. 3b). The 2007 DEM shows the early stages of the flow capture: the ice surface in the NE, in the location of the deepest section of the Jökulsárlón trench (Fig. 1b), was ~ 100 m lower than surrounding areas (Fig. 3a). Esjufjallarond and longitudinal debris folia to the south-west of it, indicate the previous ice flow direction towards the SSE (Fig. 3c). In 2007, Esjufjallarond had not undergone significant displacement, but transverse crevasses oriented SSW to NNE had opened up, indicating a $\sim 45^\circ$ change in flow towards the east-south-east (Fig. 3c), which is confirmed in the 2015 DEM, which shows only a remnant of Esjufjallarond and extensive crevassing indicating SE to ESE flow. The flow eventually resulted in a large recumbent fold in Esjufjallarond, which was displaced ~ 300 m by 2016 (Fig. 3). The hinge line of the fold in 2016 was located where ice terminates in Jökulsárlón, while the former terminal section of Esjufjallarond is still on land to the SW (Fig. 3b).

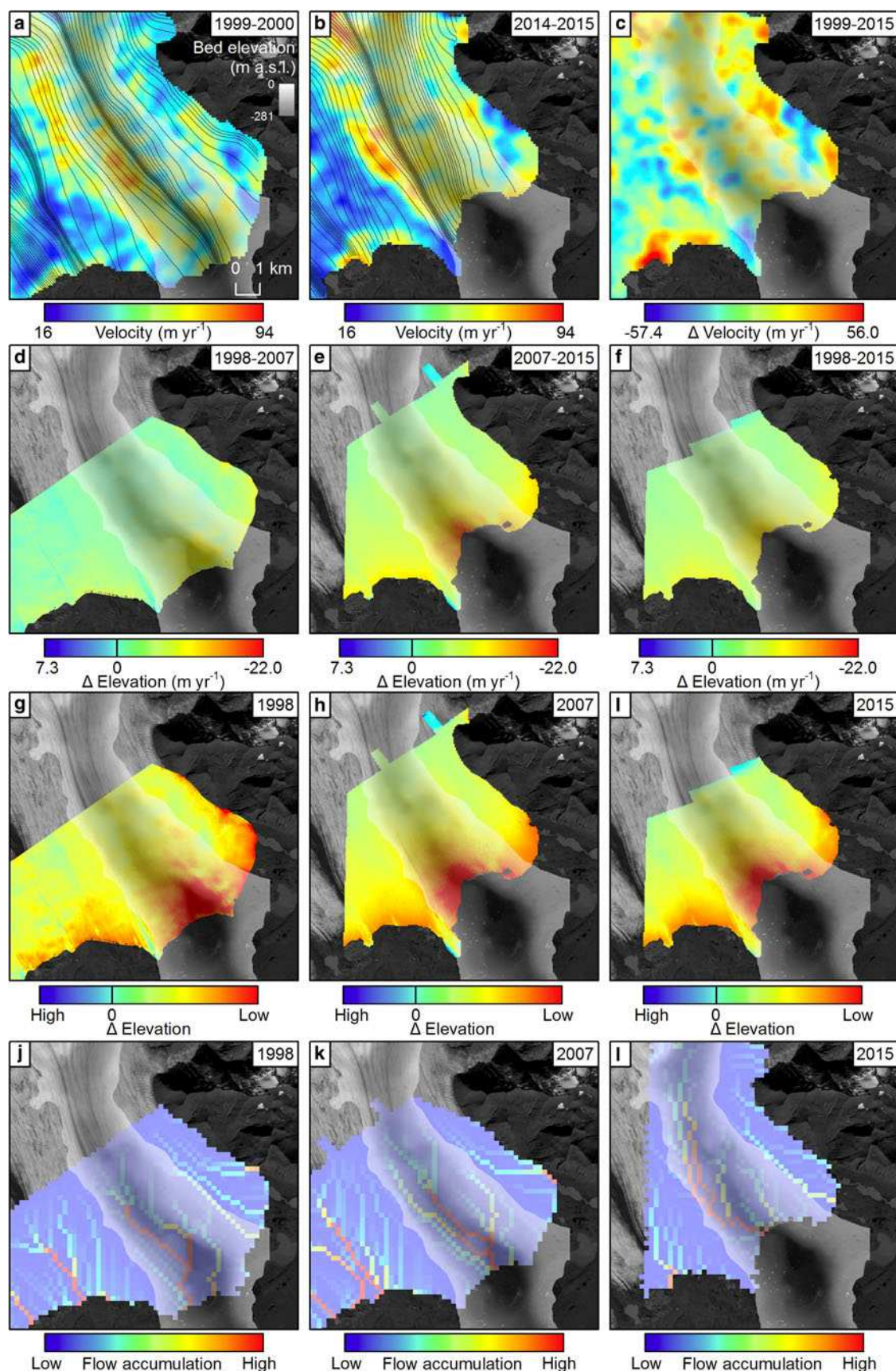


Fig. 2. Mean surface velocity, elevation and subglacial hydraulic potential changes between 1998 and 2015. Bed DEM below sea-level interpolated from digitised contours from Björnsson and others (2001). The background image is a 2015 Landsat 8 band 8 image. (a) Landsat-derived mean surface velocity for 1999–2000. Black lines are velocity-derived flowlines. (b) Landsat-derived mean surface velocity for 2014–2015. Black lines are velocity-derived flowlines. (c) Velocity change between a and b. (d) Mean annual surface elevation change between 1998 and 2007. (e) Mean annual surface elevation change between 2007 and 2015. (f) Mean annual surface elevation change between 1998 and 2015. (g) Standard deviation stretch ($n = 2.5$) of d. (h) Standard deviation stretch ($n = 2.5$) of e. (i) Standard deviation stretch ($n = 2.5$) of f. (j) Subglacial flow accumulation in 1998. (k) Subglacial flow accumulation in 2007. (l) Subglacial flow accumulation in 2015.

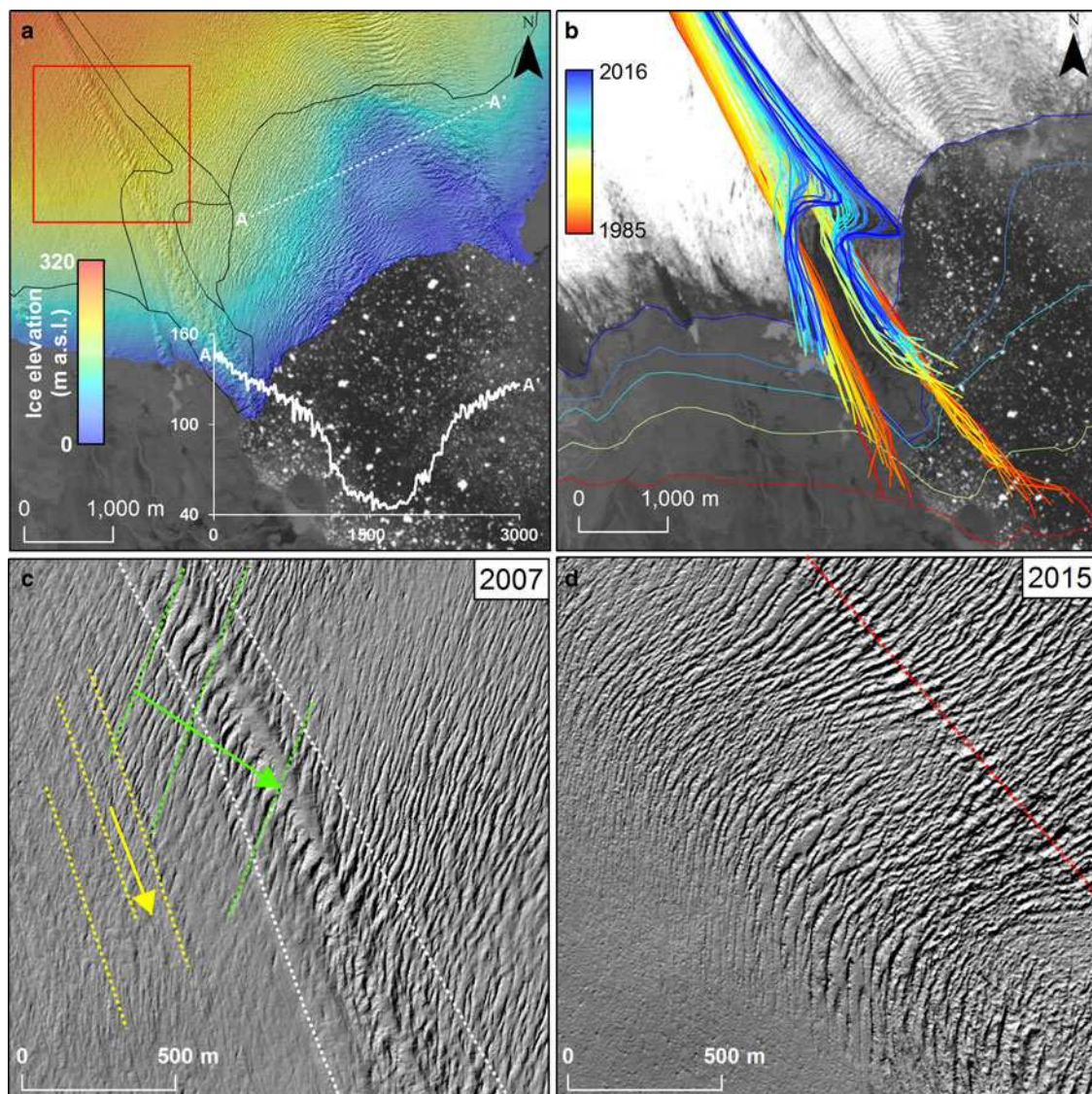


Fig. 3. (a) 2007 SfM DEM of the glacier surface. Black lines demarcate the 2016 margin and medial moraine outlines. The inset graph shows the cross profile indicated by line A-A' (in metres). The red box indicates the location of c and d. (b) Band 8 Landsat 8 ETM+ image from 13 May 2016 overlain with mapped medial moraine edge positions from 1985 to 2016. Ice margin positions in 1985, 2000, 2007, 2010 and 2016 are shown on the same colour scale. (c) 315° hillshaded 2007 DEM showing the medial moraine (outline in white), longitudinal debris folia (yellow) indicating that the initial flow direction was to the SSE, and transverse crevasses (green) which have opened up indicating the switching of flow to the ESE. (d) 315° hillshaded DEM showing the same area as c in 2015. Note the significant changes compared with the 2007 DEM. The remnant medial moraine is indicated with a red dashed line.

5. DISCUSSION AND IMPLICATIONS

As explained above, it has been suggested that flow switches can be caused by a variety of mechanisms (Winsborrow and others, 2012). We now assess whether these mechanisms may be responsible for the flow switch observed at Breiðamerkurjökull.

5.1. Accommodation space

Dowdeswell and others (2006) suggested that flow switches may occur if accommodation space is filled with sediment. Outwash from the western part of flow unit 4 is deposited in Jökulsárlón (Björnsson and others, 2001), however Jökulsárlón is too large for sediment deposition to be close to filling the available space.

5.2. Changes in basal thermal regime

Breiðamerkurjökull has not undergone significant changes in basal thermal regime over the study period, so we rule out this mechanism.

5.3. Large-scale changes in mass balance

Breiðamerkurjökull has been in a state of negative mass balance since the mid-1990s (Björnsson and Pálsson, 2008; Pálsson and others, 2014). The glacier front has been continuously retreating and the ice surface has been lowering (Figs 1, 2). We suggest that it is likely that this trend of negative mass balance is partly responsible for the observed flow switch, in combination with the subglacial topography and subglacial hydrology.

5.4. Variations in subglacial topography

The capture of part of flow unit 3 by flow unit 4 is likely controlled by bed topography. A large trench up to 300 m below sea level exists along the central axis of Jökulsárlón (Björnsson, 1996; Björnsson and others, 2001; Fig. 2), the glaciological impacts of which were identified by Evans and Twigg's (2002) map of the glacier surface depression

(see also Fig. 3a). Retreat and surface lowering have been most marked along this trench (Figs 1b, 2d–i), consistent with the water depth model of iceberg calving, which was modelled at Breiðamerkurjökull by Nick and others (2007). As ice retreats over the Jökulsárlón trench it drives faster ice flow and draws down the ice surface. This is supported by observations of higher ice velocity and surface lowering at the calving front, where the trench is deepest (Fig. 2; Voytenko and others, 2015). However, it should be noted that calving flux need not necessarily be related to velocity if the glacier is retreating (Benn and others, 2007), which is the case at Breiðamerkurjökull.

It has been demonstrated empirically that water depth exerts a strong control on ice flux, and thereby calving rates (Schoof, 2007) and water depth has been invoked as the mechanism for flow switches in fjord systems (Briner and others, 2009), marine-terminating outlet glaciers (Stokes and others, 2014) and palaeo-ice streams (Winsborrow and others, 2012). We suggest that as Breiðamerkurjökull retreats over the deepest part of the Jökulsárlón trench, flow velocity increases locally where the trench is deepest. This is likely related to calving, which in the water depth model occurs at a greater rate in deeper water (e.g. Nick and others, 2007). It is also possible that melting from incursion of warm marine water enhances calving, particularly where cold subglacial meltwater emerges from beneath the glacier (also in the deepest part of the trough: see Figs 2j–l), acting to ‘draw in’ warmer water (Voytenko and others, 2016). Increased flow velocity in turn lowers the ice surface at this location (Fig. 2). The influence of basal topography is highest at the thinnest part of the glacier, where the ratio between water depth and ice thickness is highest, which is why the most significant changes are seen as the terminus retreats over the overdeepening. Ice-surface lowering promotes drawdown of the surrounding ice, which is sufficient to deflect flow from flow unit 3 to the east, into flow unit 4, propagating the switch up-ice. This can be seen by the deviation of flowlines in Figures 2a, b, and in more detail in the deflection of Esjufjallarond (Fig. 3b) and the cross-cutting surface features in the DEM from 2007 (Fig. 3c), which shows the configuration of the glacier during the flow switch. The 2015 DEM of the same area (Fig. 3d) shows the subsequent configuration of the ice-surface post-switch, with extensive crevassing clearly portraying the new flow direction.

5.5. Subglacial hydrology

In addition to calving, subglacial meltwater flow is likely to be heavily influenced by the Jökulsárlón trench. Subglacial meltwater flow is controlled primarily by the bed slope and, to a lesser extent, the ice-surface slope (Shreve, 1972). It has been demonstrated using data from Greenland that subglacial meltwater routing can exhibit temporal variations between catchments and stimulate changes in ice dynamics (Chu and others, 2016). Subglacial hydraulic potential modelling suggests that meltwater beneath Breiðamerkurjökull will drain preferentially into the Jökulsárlón trench (Figs 2j–l). Indeed, strong meltwater currents and suspended sediment plumes indicative of subglacial runoff have been observed near the calving front (Hodgkins and others, 2016). Subglacial water pressure in the trench is likely to be high, since the deep water of Jökulsárlón provides a high base-level (Benn and Evans, 2010). High water pressures and preferential routing of water in the Jökulsárlón trench promote

increased sliding and may provide an additional explanation for the high velocity of this part of the glacier. Modelled flow accumulation follows the thalweg of the Jökulsárlón trench in all time steps (Figs 2j–l) and so is unlikely to be responsible for the flow switch by itself. Rather, it would have acted to maintain high velocity, the focus of which is ‘steered’ by the basal topography (water depth). The data presented in this paper provide observations from a modern glacier to support the notion that basal topography exerts an important control over ice dynamics (cf. Aschwanden and others, 2016). This has implications for understanding the response of ice masses to climatic warming. Basal overdeepenings, which are present beneath many parts of the Greenland (Bamber and others, 2013) and Antarctic (Fretwell and others, 2013) ice sheets, may alter ice flow vectors and promote flow switching, which may either increase or decrease retreat, depending on the intricacies of the topographic setting. As parts of these ice sheets retreat they will encounter different subglacial topography, making flow switching and concomitant changes in velocity and retreat rates likely. Thus, detailed knowledge of bed topography, and its influence on ice dynamics, is an essential source of information for predicting the fate of water-terminating ice in any setting.

SUPPLEMENTARY MATERIAL

The supplementary material for this article can be found at <http://dx.doi.org/10.1017/jog.2017.22>.

ACKNOWLEDGEMENTS

We are grateful to Chief Editor Graham Cogley and Scientific Editor Ted Scambos, as well as two anonymous reviewers, whose comments increased the clarity of the work.

¹Department of the Natural and Built Environment, Sheffield Hallam University, Sheffield, UK
ROBERT D. STORRAR¹
ANDREW H. JONES¹
DAVID J. A. EVANS²

²Department of Geography, Durham University, Durham, UK

E-mail: Robert Storrar <r.storrar@shu.ac.uk>

REFERENCES

- Anandakrishnan S and Alley RB (1997) Stagnation of ice stream C, West Antarctica by water piracy. *Geophys. Res. Lett.*, **24**, 265–268
- Aschwanden A, Fahnestock MA and Truffer M (2016) Complex Greenland outlet glacier flow captured. *Nat. Commun.*, **7**, 10524
- Bamber J and 9 others (2013) A new bed elevation dataset for Greenland. *Cryosphere*, **7**, 499–510
- Benn DI and Evans DJA (2010) *Glaciers & glaciation*. Hodder Arnold, London
- Benn DI, Hulton NRJ and Mottram RH (2007) ‘Calving laws’, ‘sliding laws’ and the stability of tidewater glaciers. *Ann. Glaciol.*, **46**, 123–130
- Björnsson H (1996) Scales and rates of glacial sediment removal: a 20 km long and 300 m deep trench created beneath Breiðamerkurjökull during the Little Ice Age. *Ann. Glaciol.*, **22**, 141–146
- Björnsson H and Pálsson F (2008) Icelandic glaciers. *Jökull*, **58**, 365–386

- Björnsson H, Pálsson F and Guðmundsson S (2001) Jökulsárlón at Breiðamerkursandur, Vatnajökull, Iceland: 20th century changes and future outlook. *Jökull*, **50**, 1–18
- Briner JP, Bini AC and Anderson RS (2009) Rapid early Holocene retreat of a Laurentide outlet glacier through an Arctic fjord. *Nat. Geosci.*, **2**, 496–499
- Conway H and 5 others (2002) Switch of flow direction in an Antarctic ice stream. *Nature*, **419**, 465–467
- Dowdeswell JA, Ottesen D and Rise L (2006) Flow switching and large-scale deposition by ice streams draining former ice sheets. *Geology*, **34**, 313–316
- Evans DJA and Twigg DR (2000) Breiðamerkurjökull 1998. 1: 30,000 Scale Map. University of Glasgow and Loughborough University.
- Evans DJA and Twigg DR (2002) The active temperate glacial land-system: a model based on Breiðamerkurjökull and Fjallsjökull, Iceland. *Quat. Sci. Rev.*, **21**, 2143–2177
- Favier L and 8 others (2014) Retreat of Pine Island Glacier controlled by marine ice-sheet instability. *Nat. Clim. Change*, **4**, 117–121
- Fretwell P and 9 others (2013) Bedmap2: improved ice bed, surface and thickness datasets for Antarctica. *Cryosphere*, **7**, 375–393
- Hodgkins R, Bryant R, Darlington E and Brandon M (2016) Pre-melt-season sediment plume variability at Jökulsárlón, Iceland, a preliminary evaluation using in-situ spectroradiometry and satellite imagery. *Ann. Glaciol.*, **57**, 1–8
- Hooke RL (1984) On the role of mechanical energy in maintaining subglacial water conduits at atmospheric pressure. *J. Glaciol.*, **30**, 180–187
- Hulbe CL and Fahnestock MA (2004) West Antarctic ice-stream discharge variability: mechanism, controls and pattern of grounding-line retreat. *J. Glaciol.*, **50**, 471–484
- Jacobel RW, Scambos TA, Raymond CF and Gades AM (1996) Changes in the configuration of ice stream flow from the West Antarctic Ice Sheet. *J. Geophys. Res.: Solid Earth*, **101**, 5499–5504
- Kääb A and Vollmer M (2000) Surface geometry, thickness changes and flow fields on creeping mountain Permafrost: automatic extraction by digital image analysis. *Permafrost Periglacial Process.*, **11**, 315–326
- Livingstone SJ, Clark CD, Woodward J and Kingslake J (2013) Potential subglacial lakes and meltwater drainage pathways beneath the Antarctic and Greenland ice sheets. *Cryosphere*, **7**, 1721–1740
- Nick FM, Van der Kwast J and Oerlemans J (2007) Simulation of the evolution of Breiðamerkurjökull in the late Holocene. *J. Geophys. Res.-Solid Earth*, **112**, B01103/01101–B01103/01112
- Ó Cofaigh C, Evans DJA and Smith IR (2010) Large-scale reorganization and sedimentation of terrestrial ice streams during late Wisconsinan Laurentide Ice Sheet deglaciation. *Geol. Soc. Am. Bull.*, **122**, 743–756
- Pálsson F, Gunnarsson A, Jónsson Þ, Steinþórsson S and Pálsson HS (2014) Vatnajökull: mass balance, meltwater drainage and surface velocity of the glacial year 2012–13. *Landsvirkjun*, LV-2014-068
- Payne A and Dongelmans P (1997) Self-organization in the thermo-mechanical flow of ice sheets. *J. Geophys. Res.: Solid Earth*, **102**, 12219–12233
- Pfeffer WT (2007) A simple mechanism for irreversible tidewater retreat. *J. Geophys. Res.*, **112**, F03S25
- Retzlaff R and Bentley CR (1993) Timing of stagnation of Ice Stream C, West Antarctica, from short-pulse radar studies of buried surface crevasses. *J. Glaciol.*, **39**, 553–561
- Schoof C (2007) Ice sheet grounding line dynamics: steady states, stability, and hysteresis. *J. Geophys. Res.: Earth Surf.* (2003–2012), **112**
- Shreve RL (1972) Movement of water in glaciers. *J. Glaciol.*, **11**, 205–214
- Stokes CR and Tarasov L (2010) Ice streaming in the Laurentide Ice Sheet: a first comparison between data-calibrated numerical model output and geological evidence. *Geophys. Res. Lett.*, **37**, L01501
- Stokes CR, Clark CD and Storrar RD (2009) Major changes in ice stream dynamics during deglaciation of the north-western margin of the Laurentide Ice Sheet. *Quat. Sci. Rev.*, **28**, 721–738
- Stokes CR, Corner GD, Winsborrow MC, Husum K and Andreassen K (2014) Asynchronous response of marine-terminating outlet glaciers during deglaciation of the Fennoscandian Ice Sheet. *Geology*, **42**, 455–458
- Storrar RD, Evans DJA, Stokes CR and Ewertowski M (2015) Controls on the location, morphology and evolution of complex esker systems at decadal timescales, Breiðamerkurjökull, SE Iceland. *Earth Surf. Process. Landforms*, **40**, 1421–1438
- Syverson KM, Gaffield SJ and Mickelson DM (1994) Comparison of esker morphology and sedimentology with former ice-surface topography, Burroughs Glacier, Alaska. *Geol. Soc. Am. Bull.*, **106**, 1130–1142
- Thomas RH (1979) The dynamics of marine ice sheets. *J. Glaciol.*, **24**, 167–177
- Voytenko D and 7 others (2015) Multi-year observations of Breiðamerkurjökull, a marine-terminating glacier in southeastern Iceland, using terrestrial radar interferometry. *J. Glaciol.*, **61**, 42–54
- Weertman J (1974) Stability of the junction of an ice sheet and an ice shelf. *J. Glaciol.*, **13**, 3–11
- Winsborrow MC, Stokes CR and Andreassen K (2012) Ice-stream flow switching during deglaciation of the southwestern Barents Sea. *Geol. Soc. Am. Bull.*, **124**, 275–290

MS received 12 July 2016 and accepted in revised form 28 March 2017